Lymphoma endothelium preferentially expresses Tim-3 and facilitates the progression of lymphoma by mediating immune evasion

Xiaoyuan Huang, Xiangyang Bai, Yang Cao, Jingyi Wu, Mei Huang, Duozhuang Tang, Si Tao, Tao Zhu, Yanling Liu, Yang Yang, Xiaoxi Zhou, Yanxia Zhao, Mingfu Wu, Juncheng Wei, Daowen Wang, Gang Xu, Shixuan Wang, Ding Ma, and Jianfeng Zhou

Cancer Biology Research Center, Tongji Hospital, Tongji Medical College, Huazhong University of Science and Technology, Wuhan, Hubei 430030, China

Angiogenesis is increasingly recognized as an important prognosticator associated with the progression of lymphoma and as an attractive target for novel modalities. We report a previously unrecognized mechanism by which lymphoma endothelium facilitates the growth and dissemination of lymphoma by interacting with circulated T cells and suppresses the activation of $CD4^+$ T cells. Global gene expression profiles of microdissected endothelium from lymphoma and reactive lymph nodes revealed that T cell immunoglobulin and mucin domain–containing molecule 3 (Tim-3) was preferentially expressed in lymphoma-derived endothelial cells (ECs). Clinically, the level of Tim-3 in B cell lymphoma endothelium was closely correlated to both dissemination and poor prognosis. In vitro, $Tim\text{-}3^+$ ECs modulated T cell response to lymphoma surrogate antigens by suppressing activation of $CD4^+$ T lymphocytes through the activation of the interleukin-6–STAT3 pathway, inhibiting Th1 polarization, and providing protective immunity. In a lymphoma mouse model, Tim-3–expressing ECs promoted the onset, growth, and dissemination of lymphoma by inhibiting activation of $CD4^+$ T cells and Th1 polarization. Our findings strongly argue that the lymphoma endothelium is not only a vessel system but also a functional barrier facilitating the establishment of lymphoma immune tolerance. These findings highlight a novel molecular mechanism that is a potential target for enhancing the efficacy of tumor immunotherapy and controlling metastatic diseases.

CORRESPONDENCE
Ding Ma:
dma@tjh.tjmu.edu.cn
OR
Jianfeng Zhou:
jfzhou@tjh.tjmu.edu.cn

Abbreviations used: CBA, cytokine bead assay; CHO, Chinese hamster ovary; DLBCL, diffuse large B cell lymphoma; DTH, delayed type hypersensitivity; EC, endothelial cell; IPI, international prognosis index; LCM, laser capture microdissection; LDH, lactate dehydrogenase; MOI, multiplicity of infection; MVD, microvessel density; p-STAT3, phosphorylated STAT3; sTim-3, soluble Tim-3; Tim-3, T cell Ig and mucin domain–containing molecule 3; TT, tetanus toxin; UVEC, umbilical vein EC; VEGF, vascular endothelial growth factor.

Angiogenesis is increasingly being recognized as an important prognostic factor associated with the progression of lymphoma and as an attractive target for next generation treatment modalities (Bruns et al., 2005; Koster and Raemaekers, 2005; Lenz et al., 2008). However, our understanding of lymphoma angiogenesis is still in its infancy. Some recent studies have demonstrated that lymphoma vessels are far more complex than initially perceived. Apart from being structurally different from normal blood vessels, lymphoma microvessels possess neoplasm-specific gene alterations. For example, lymphoma-specific chromosomal translocations were detected in 15–85% of microvascular endothelial cells (ECs) from patients with B cell lymphoma (Streubel et al., 2004). Given that cytogenetic abnormalities confer upon lymphoma cells the ability to initiate malignancy and promote survival and proliferation, the presence of these abnormalities in lymphoma ECs might make lymphoma microvessels active contributors to tumor progression and dissemination, rather than simply conduits for nutrients and oxygen. Therefore, we hypothesized that lymphoma microvessels might possess some unique

X. Huang, X. Bai, and Y. Cao contributed equally to this paper.

The Rockefeller University Press $30.00
J. Exp. Med. Vol. 207 No. 3 505-520
www.jem.org/cgi/doi/10.1084/jem.20090397

The Journal of Experimental Medicine

molecular aberrations that actively promote the progression of lymphoma.

One strategy to identify tumor-specific molecular abnormalities is to use global gene expression analysis techniques (Neri and Bicknell, 2005). However, a very limited number of studies have been done to compare the global gene expression profile associated with lymphomas versus reactive lymph node vessels. However, we recently developed a method for the analysis of global gene expression in microvessels obtained from primary lymph node samples (Bai et al., 2008). The microvessels are isolated by laser capture microdissection (LCM) from lymph nodes fixed in situ and subjected to microarray analysis. This method has proven to be a powerful tool for identifying molecular details of microvessels in situ. In the present study, we used this technique to compare the gene expression profiles of microvessels from lymphomas versus reactive lymph nodes. Unexpectedly, we identified the expression of a transcript called T cell Ig and mucin domain–containing molecule 3 (Tim-3), also known as hepatitis A virus cellular receptor 2, in microvessels of lymphomas but not in reactive lymph nodes. Because it has previously been demonstrated that Tim-3 is preferentially expressed in differentiated Th1 cells and promotes immunological tolerance (Kuchroo et al., 2003; Sabatos et al., 2003; Sánchez-Fueyo et al., 2003; Zhu et al., 2005), we examined expression profiles of Tim-3 in microvessels from lymphoma samples, which underscored the potential role of endothelium-expressed Tim-3 in the immune evasion and progression of lymphoma.

RESULTS

Transcriptional profiles of lymphoma endothelium revealed unexpected expression of Tim-3

To identify potential molecular aberrations in the lymphoma endothelium, lymph nodes from 13 patients were collected at the time of surgery for diagnostic purposes. Endothelium was isolated from the samples, and mRNA was extracted. The RNA samples were used for subsequent GeneChip probe arrays if contamination of lymphoid tissues could be excluded. Five lymph node samples (including two diffuse large B cell lymphomas [DLBCLs], one peripheral T cell lymphoma, and two reactive lymph nodes) were confirmed with good purity and were subjected to microarray analysis (Fig. 1 A). Around 3,000 transcripts were present in each sample examined. Among them, several well-known vascular markers such as CD144, von Willebrand factor, and CD105 were detected. 13 transcripts were found to be at least twofold more abundant in reactive lymph node–derived endothelium than in lymphoma-derived endothelium (Fig. 1 B). 14 transcripts, on the other hand, were found to be at least twice as abundant in lymphoma-derived endothelium than in reactive lymph node–derived endothelium (Fig. 1 B). These genes covered a wide range of cellular functions, such as regulation of vascular endothelial growth factor (VEGF) mRNA stability (Shih and Claffey, 1999; Song et al., 2002). However, we were intrigued by the unexpected finding that expression of Tim-3 was more than twofold higher in lymphoma-derived endothelium, because it has been extensively documented that Tim-3 is preferentially expressed in differentiated Th1 cells, regulates Th1 responses, and induces peripheral immune tolerance (Kuchroo et al., 2003; Sabatos et al., 2003; Sánchez-Fueyo et al., 2003; Zhu et al., 2005). We thus selected Tim-3 for further study to investigate whether it is preferentially expressed in

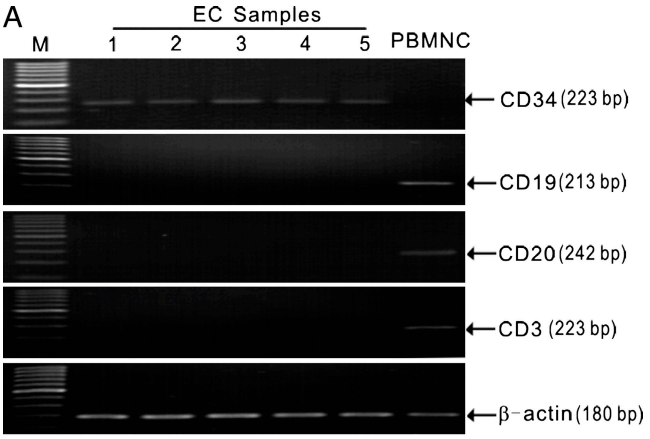

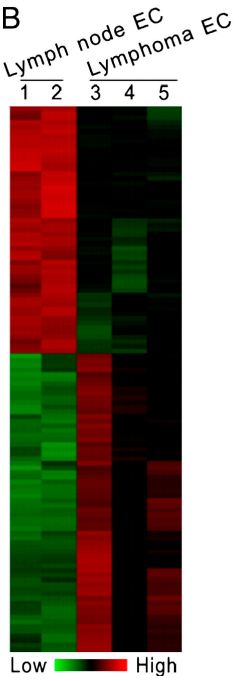

Abundant in Lymphoma EC

Gene symbol	Increased folds
RPS3A	8.67
AP3M1	6.66
POLH	2.90
SORCS2	2.89
FAM112B	2.69
HAVCR2 (Tim-3)	2.46
HERV-FRD	2.15
C7orf19	2.03
DKFZP686P18101	1.91
HNRPL	1.85
Similar to E74-like factor isoform 1; new Ets-related factor	1. 70
CHST11	1.67
TPP1	1.39
SET	1.29

Abundant in reactive lymph node EC

Gene symbol	Increased folds
CNR1	8.11
KIAA0415	4.85
ARID4B	4.49
HBB	4.13
SLC7A11	3.08
DAG1	3.04
HNMT	3.00
SMAD4	2.89
PRKACB	2.77
ISL1	2.68
IQCB1	2.17
DMC1	1.68
RBM18	1.40

Figure 1. Transcriptional profiles of lymphoma endothelium. (A) Evaluation of purity of LCM-isolated ECs before GeneChip probe arrays. Five samples were used for subsequent GeneChip probe arrays. In these samples, the endothelial marker CD34 showed robust amplification only in the endothelium fraction. However, the contamination of nonendothelium tissues was excluded because no T or B lymphocyte markers were detected. (B) Comparison of the global gene expression profiles associated with lymphomas versus reactive lymph node vessels. (left) Heat maps were developed with the GeneSpring hierarchical clustering algorithm after eliminating all genes for which the difference in the means was less than the SE of the difference of means between groups. (right) List of genes and expressed sequence tags overexpressed in LCM-isolated endothelium from lymphoma or reactive lymph node samples.

lymphoma-derived ECs, as well as what the functional significance of Tim-3 expression might be.

Tim-3 is preferentially expressed in lymphoma-derived ECs

Given the heterogeneity of lymphomas, we first validated the microarray data by performing in situ hybridization on lymphoma cryosections ($n = 10$) or reactive lymph nodes ($n = 10$). Tim-3 mRNA was not detected in the endothelium in the majority of reactive lymph nodes; weakly stained Tim-3 mRNA was only detected in the endothelium of 2 out of the 10 non-neoplastic lymph nodes. In contrast, strong staining of Tim-3 mRNA was detected in the endothelium in 8 out of 10 lymphoma specimens (Fig. 2 A). Furthermore, positive endothelium staining for Tim-3 protein was detected in only 10.34% (3 out of 29) of reactive lymph nodes (Fig. 2 B), but positive staining was detected in ~52.38% (55 out of 105) of the lymphoma specimens examined. When the endothelium-expressed Tim-3 protein was further compared by semiquantitative immunoreactivity H-scoring, lymphoma endothelium displayed a much higher Tim-3 score than reactive lymph nodes (1.085 ± 0.822 vs. 0.229 ± 0.396; $P < 0.001$).

Next, we purified ECs from lymph nodes of lymphoma ($n = 10$) or reactive lymph nodes ($n = 2$), and the EC purity was confirmed (Fig. 2, C and D). ECs from 7 out of 10 lymphoma tissues stained strongly for Tim-3 protein on the cell membrane (Fig. 2 E). Conversely, ECs from the two reactive lymph nodes examined were negative for Tim-3. It was previously reported that Tim-3 mRNA is alternatively spliced to produce two mRNA transcripts in mice, although no such data are currently available in humans. The full-length transcript

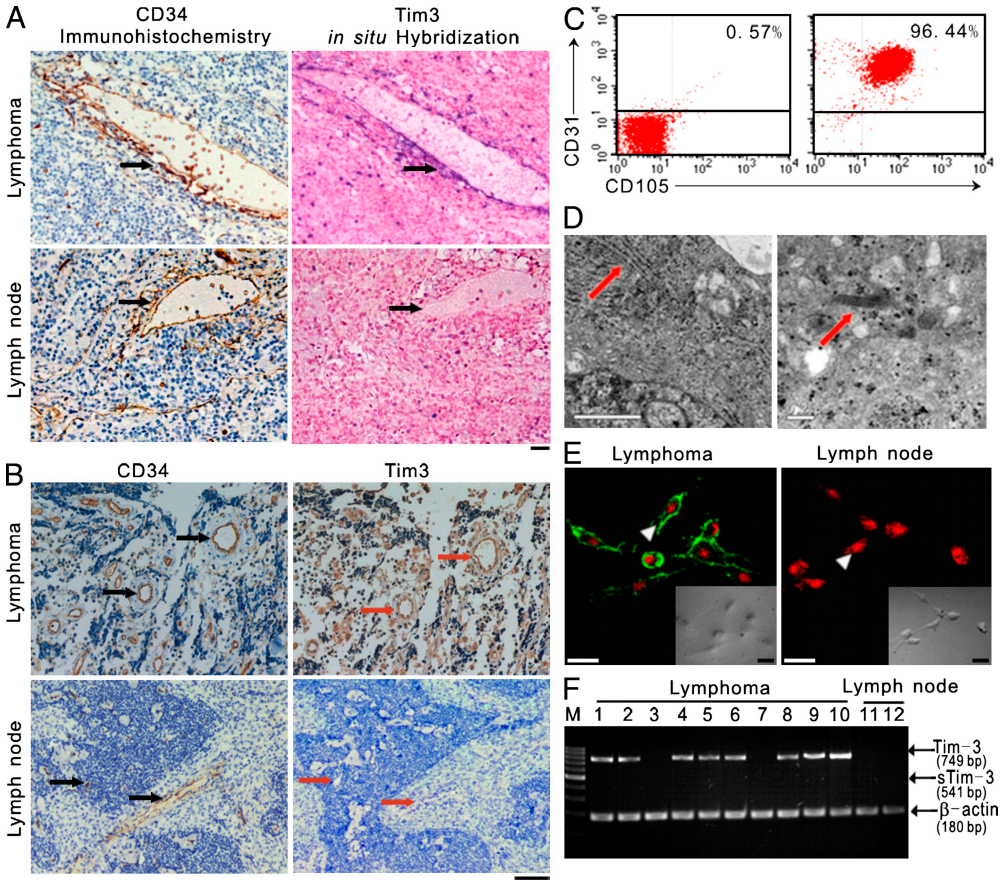

Figure 2. Tim-3 is preferentially expressed on lymphoma-derived ECs. (A) In situ hybridization of cryosections of lymph nodes of lymphoma or reactive lymph nodes. (left) CD34-positive microvessels in lymphomas or reactive lymph nodes (brown; arrows). (right) Tim-3 transcripts (blue) were detected in microvessels (arrows) in lymphomas but not in reactive lymph nodes. Bar, 20 µm. (B) Immunohistochemical staining of CD34 (left) and Tim-3 (right) proteins. Immunoreactive Tim-3 (red arrows) was readily detectable in the endothelium (black arrows) of lymphoma but not in reactive lymph node endothelium. Bar, 20 µm. (C) ECs purified from lymph nodes of lymphoma or reactive lymph nodes. Isolated ECs were costained with antibodies against CD31 and CD105. Cells were analyzed by flow cytometry. (right) The isolated ECs were found to be >95% pure. (left) Antibody isotype control. Similar results were observed in three independent experiments. (D) Isolated ECs viewed by transmission electron microscopy. The ECs contained plentiful endoplasmic reticulum in the cytoplasm (left, arrow), and Weible-Palade bodies were observed (right, arrow). Bars: (left) 1 µm; (right) 0.2 µm. (E) ECs purified from lymphomas (left) and reactive lymph nodes (right) stained with an immunofluorescent anti–Tim-3 antibody and observed with a confocal laser scanning microscope. Tim-3 protein (green; arrowhead) is in the cell membranes of lymphoma ECs. Cell nuclei (red; arrowhead) were visualized by staining with propidium iodide. Bars, 100 µm. (F) RT-PCR of Tim-3 mRNA and sTim-3 mRNA from 10 lymphoma samples and 2 reactive lymph node samples.

encodes Tim-3, whereas the shorter one lacks the mucin and transmembrane domain and is speculated to encode soluble Tim-3 (sTim-3; Geng et al., 2006). The sTim-3 protein was previously proposed to be an inhibitory molecule in the T cell–mediated immune response and was shown to promote cancer growth in tumor-bearing mice (Geng et al., 2006). To address whether lymph node ECs produced two isoforms of Tim-3, mRNA from freshly purified lymph node ECs was subjected to PCR analysis. Although a full-length Tim-3 transcript was detected in ECs from 8 out of 10 lymphoma samples, the shorter Tim-3 transcript was not detected in any of the 10 samples, and ECs from two reactive lymph nodes were negative for all Tim-3 isoforms (Fig. 2 F).

Interestingly, the unexpected expression of Tim-3 was also observed in microvessels of breast cancer samples. Positive endothelium staining for Tim-3 protein was detected in only 14.3% (2 out of 12) of mastopathia samples (Fig. S1). In contrast, positive staining of Tim-3 protein was detected in ∼48.2% (29 out of 56) of the breast cancer specimens examined. When endothelium-expressed Tim-3 protein was further compared by semiquantitative immunoreactivity H-scoring, breast cancer endothelium displayed a much higher Tim-3 score than mastopathia (2.438 ± 2.258 vs. 0.583 ± 1.144; $P < 0.001$).

Tim-3 expression in the endothelium is correlated with local immune profiles and adverse clinical features of lymphoma

We initially evaluated the correlation of Tim-3 expression with microvessel density (MVD) in lymphoma samples (Fig. 3 A). Endothelial Tim-3 protein levels were found to significantly correlate with the MVD of lymphoma ($r = 0.446$; $P < 0.001$). Next, we examined the potential correlation of Tim-3$^+$ ECs (CD34$^+$Tim-3$^+$) with CD4$^+$Tim-3$^+$ T cells. The presence of Tim-3–expressing ECs did not appear to influence the percentage of CD4$^+$Tim-3$^+$ T cells observed either in vitro or in vivo (Fig. S2). To study the possible correlation of Tim-3 expression with local immune profiles in lymphoma sections, 12 cases of endothelial Tim-3–positive or –negative DLBCLs were randomly selected and compared for the dendritic cells expressing CD1a (Fig. 3 B) and subsets of T cells expressing CD4, CD8, or CD4 and CD8 (Fig. 3, C–E). Tim-3–positive DLBCLs had a significantly lower percentage of CD4$^+$ T cells (4.41% ± 6.87% vs. 11.3% ± 7.51%; $P = 0.03$) and a lower CD4/CD8 ratio (0.23 ± 0.32 vs. 0.79 ± 0.49; $P = 0.003$; Fig. 3 C) when compared with Tim-3–negative DLBCLs. There was no significant difference, however, in the percentage of CD8 and CD1a expression between Tim-3–positive and –negative DLBCLs ($P > 0.05$). These data strongly imply that endothelial Tim-3 expression in lymphoma might affect CD4$^+$ but not CD8$^+$ T cells or CD1a$^+$ dendritic cells in vivo. To determine whether endothelium-expressed Tim-3 correlates with clinical features of lymphoma, 85 cases of lymphoma with complete medical records were selected for analysis (Table I). No correlation was found between Tim-3 levels and gender, age, or histological origins (T or B cell lymphoma). However, high Tim-3 expression was statistically correlated with higher lymphoma stages ($P = 0.043$), B symptoms (i.e., fever, night sweats, and weight loss; $P = 0.037$), and higher international prognosis index (IPI) scores ($P = 0.002$). Because of the well-known differences in the biological and clinical behavior between

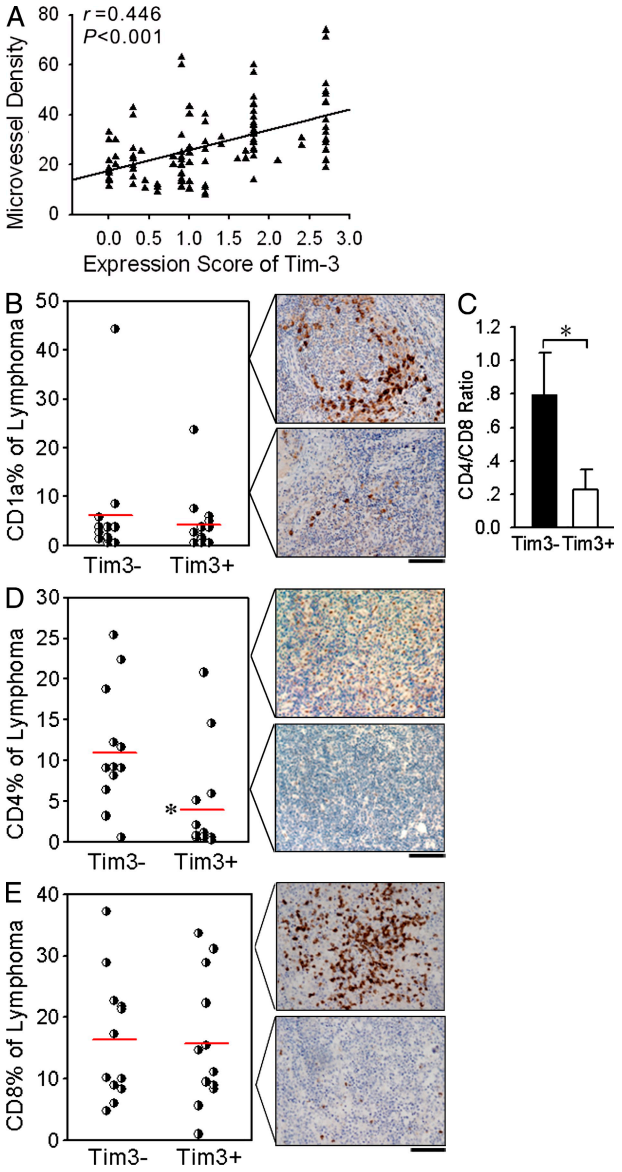

Figure 3. Tim-3–expressing endothelium in lymphomas correlates with local immune profiles. (A) Scatter plot showing Tim-3 expression versus MVD in 105 lymphoma samples. MVD in lymphoma sections significantly correlated with levels of Tim-3 protein in the endothelium, as defined by immunoreactivity scores ($r = 0.446$; $P < 0.001$). (B) Mean (red lines) of CD1a$^+$ dendritic cells. (top right) A typical image represents higher CD1a$^+$ expression than the mean percentage. (bottom right) A typical image represents lower CD1a$^+$ expression than the mean percentage. (C) CD4$^+$/CD8$^+$ cell ratio for Tim-3–negative ($n = 12$) and Tim-3–positive ($n = 12$) DLBCLs. Data are presented as means ± SD of at least three experiments. (D) CD4$^+$ T cell and (E) CD8$^+$ T cell populations are presented as a percentage of total lymph node cells. Representative images of the lymphocyte population (brown; stained with antibody against CD1a$^+$, CD4$^+$, or CD8$^+$) appear to the right of each graph. Bars, 50 µm. *, $P < 0.01$.

T and B cell lymphomas, we further analyzed the possible correlation between endothelium-expressed Tim-3 and the clinical features of T or B cell lymphoma in a separate analysis. Interestingly, high Tim-3 expression was statistically correlated with higher lymphoma stages (P = 0.002), B symptoms (P = 0.014), and higher IPI scores (P = 0.001) only in B cell lymphoma (Table I).

Validation of a cell model for studying interactions between ECs and autologous T lymphocytes

To study the direct effects of Tim-3–expressing ECs on lymphocytes, we established a cell model based on several previous findings. First, ECs can act as semiprofessional APCs to process and present antigens to T cells (Choi et al., 2004; Danese et al., 2007). Second, lymphoma ECs harbor lymphoma-specific chromosomal translocations (Streubel et al., 2004), which may serve as tumor-specific antigens. Third, a DNA fusion antigen created by fusing the N-terminal domain of fragment C of tetanus toxin (TT) with a portion of the second domain induces strong CTL responses, and thus can be used as a surrogate lymphoma antigen (Rice et al., 2001; Padua et al., 2003).

Our first step in creating the cell model was constructing an adenoviral DNA vaccine, named ADV-TT (Fig. 4 A). ADV-TT expresses a transgene that contains the N-terminal domain of fragment C of TT and a portion of the second

Table I. Tim-3–expressing endothelium correlates with clinical features of lymphoma

Features		Cases	Tim-3		
			Score[a]	*t*	p-value
Total lymphoma					
Gender	Male	54	0.994 ± 0.677	0.842	0.402
	Female	31	1.125 ± 0.721		
Age	≤40 yr	42	0.944 ± 0.71	1.289	0.201
	>40 yr	43	1.137 ± 0.667		
Clinical stage	I+II	42	0.889 ± 0.604	2.056	0.043
	III+IV	43	1.191 ± 0.745		
A&B symptoms	A	34	0.849 ± 0.688	2.136	0.037
	B	51	1.17 ± 0.67		
Histology	B	48	1.026 ± 0.705	0.359	0.72
	T	37	1.081 ± 0.684		
IPI	<2	11	0.477 ± 0.529	3.646	0.002
	≥2	74	1.125 ± 0.676		
B cell lymphoma					
Gender	Male	32	1.017 ± 0.711	0.114	0.91
	Female	16	1.042 ± 0.715		
Age	≤40 yr	23	0.967 ± 0.697	0.545	0.588
	>40 yr	25	1.079 ± 0.722		
Clinical stage	I+II	28	0.755 ± 0.585	3.412	0.002
	III+IV	20	1.405 ± 0.695		
A&B symptoms	A	27	0.814 ± 0.721	2.547	0.014
	B	21	1.298 ± 0.594		
IPI	<2	11	0.477 ± 0.529	3.667	0.001
	≥2	37	1.189 ± 0.672		
T cell lymphoma					
Gender	Male	22	0.959 ± 0.638	1.083	0.288
	Female	15	1.213 ± 0.741		
Age	≤40 yr	19	0.916 ± 0.745	1.363	0.182
	>40 yr	18	1.217 ± 0.593		
Clinical stage	I+II	14	1.157 ± 0.569	0.654	0.517
	III+IV	23	1.004 ± 0.75		
A&B symptoms	A	7	0.986 ± 0.573	0.373	0.716
	B	30	1.08 ± 0.714		
IPI	<2	0			
	≥2	37	1.062 ± 0.683		

[a]Expression score (mean ± SE). The expression score represents the expression level of Tim-3 protein in endothelium as calculated by the immunoreactivity scoring system. Corresponding *t* values and p-values are displayed for each cross tabulation.

domain. To mimic lymphoma ECs, human umbilical vein ECs (UVECs) were infected with ADV-TT to express the transgene (Fig. 4 A). The infected UVECs were then incubated with lymphocytes from the same donor (autologous lymphocytes) in the presence or absence of Tim-3 expression. Next, we checked whether MHC and co-stimulatory molecules were expressed in the UVECs (Fig. 4 B), and they were found to constitutively express MHC class I and CD58 molecules. After pretreatment with IFN-γ, MHC class II (but not CD86) molecules were detected on UVECs. These data demonstrated that, after pretreatment with IFN-γ, UVECs expressed the MHC and co-stimulatory molecules necessary for presenting antigens to both $CD4^+$ and $CD8^+$ T cells. On the other hand, infection of IFN-γ–pretreated UVECs with ADV–Tim-3 did not alter the expression of the MHC and co-stimulatory molecules (Fig. 4 B). When co-cultured, ADV-TT–infected UVECs stimulated autologous lymphocytes to proliferate in an ADV-TT dose-dependent fashion. The activation of lymphocytes appeared to be, for the most part, TT dependent, because ADV-GFP triggered a much lower level of lymphocyte proliferation (Fig. 4 C).

To further address whether the antigen-presenting function of UVECs to $CD4^+$ T cells was specific, MHC class II–positive cells (i.e., the human bronchial epithelial cell line BEAS) were used as a control. After pretreatment with IFN-γ, MHC class II molecules were detected on BEAS. Although ADV-TT–infected UVECs stimulated autologous lymphocytes to proliferate (4.75 ± 0.58), ADV-TT–infected BEAS was not able to induce HLA-A2–matched lymphocyte proliferation (1.61 ± 0.33; $P < 0.01$; Fig. 4 D). To rule out the possibility that differential lymphocyte proliferation was caused by the influence of ADV-TT on UVECs, we analyzed the effect of ADV-TT infection on UVEC proliferation and survival. ADV-TT infection did not lead to an increase in UVEC cell numbers when compared with the UVEC/PBS control (Fig. 4 E). At a multiplicity of infection (MOI) of 250,

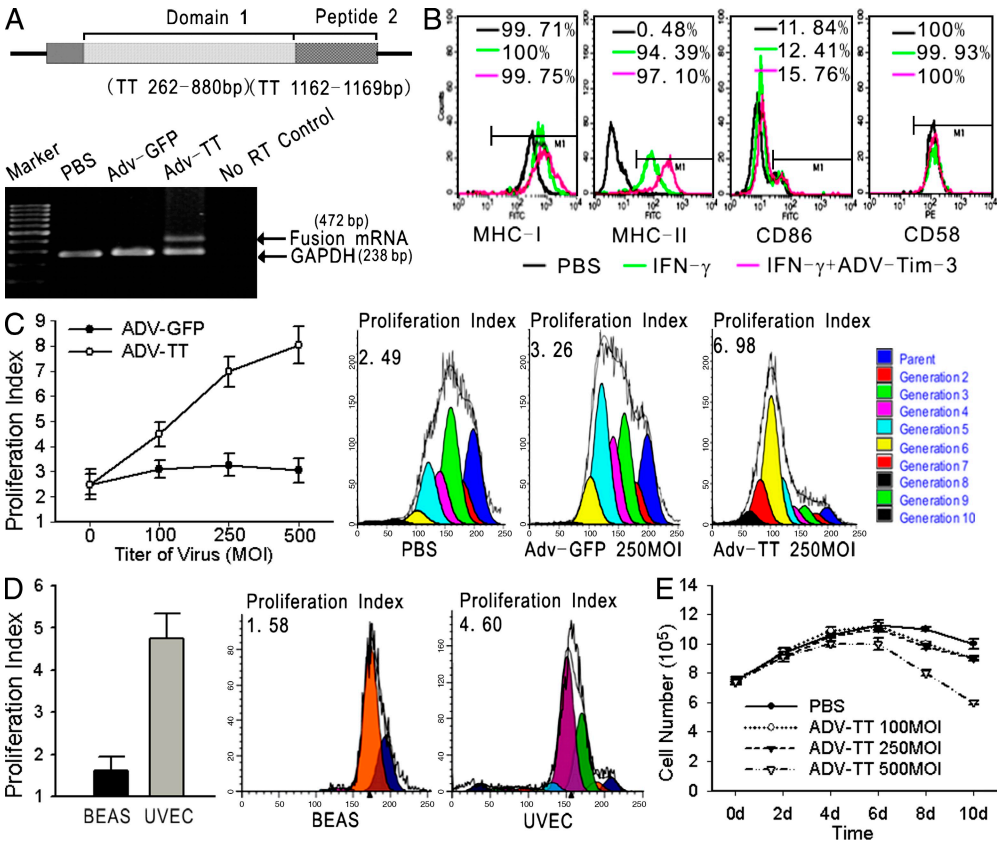

Figure 4. Validation of an in vitro cell model for studying interactions between ECs and autologous T lymphocytes. (A, top) Schematic of the ADV-TT construct. (bottom) Transcripts of TT in ADV-TT–infected UVECs were detected by RT-PCR. ADV-GFP and PBS were included as negative controls. (B) Expression of MHC class I, MHC class II, CD86, or CD58 in freshly isolated UVECs treated with PBS (black), IFN-γ (green), or IFN-γ + ADV–Tim-3 (red). (C) UVECs were infected with ADV-TT or ADV-GFP and incubated with CFSE-labeled autologous lymphocytes. The proliferation of lymphocytes was measured by FACS. (right) CFSE profiles of lymphocytes treated with ADV-GFP or ADV-TT. Data are represented as means ± SD of triplicates. (D) BEAS and UVECs were infected with ADV-TT at an MOI of 250 and incubated with CFSE-labeled autologous lymphocytes. The proliferation of lymphocytes was measured by FACS. (right) CFSE profiles of lymphocytes treated with ADV-TT. Data are represented as means ± SD of triplicates. (E) Cell proliferation of UVECs infected with various titers of ADV-TT. Infection of ADV-TT did not lead to an increase in UVEC cell numbers compared with infection with ADV-GFP or at any of the MOIs examined. Data are represented as means ± SD of triplicates. Similar results were observed in four (B) or three (C–E) independent experiments.

ADV-TT–infected UVECs significantly activated T lymphocytes with a minor cell death response (unpublished data); thus, this concentration was used in the following experiments.

In the first experiment with our cell model, we analyzed the proliferation of $CD4^+$ and $CD8^+$ T cells induced by ADV-TT–infected UVECs (Table S1). Upon exposure to ADV-TT–infected UVECs, the $CD4^+$ cell number increased to $13.16 \pm 1.59 \times 10^5$ cells/well, much higher than that of the PBS ($8.95 \pm 1.35 \times 10^5$ cells/well) or ADV-GFP–infected ($9.14 \pm 1.88 \times 10^5$ cells/well) UVEC control groups ($P < 0.05$). In the same experiment, the $CD8^+$ cell number also increased moderately in response to ADV-TT–infected UVECs ($0.83 \pm 0.15 \times 10^5$ cells/well) when compared with the PBS ($0.61 \pm 0.09 \times 10^5$ cells/well) and ADV-GFP–infected ($0.69 \pm 0.12 \times 10^5$ cells/well) UVEC control groups ($P < 0.05$). These data demonstrated that surrogate antigen TT-expressed UVECs activated both $CD4^+$ and $CD8^+$ T lymphocytes, and thus can be used as a cell model to investigate the direct effects of Tim-3–expressing ECs on T lymphocytes.

Tim-3–expressing ECs suppressed antigen-induced activation of $CD4^+$ T cells through activation of the IL-6–STAT3 pathway and provided protective immunity

UVECs were infected with ADV–Tim-3 to ectopically express Tim-3 (Fig. 5 A). As expected, the lymphocyte proliferation in response to ADV-TT–infected UVECs was significantly suppressed by ADV–Tim-3 in a dose-dependent fashion (Fig. 5, B and C). To explore whether ADV-TT led to expansion of a specific T cell clone, we used Biomed-2 multiplex TCR PCR to analyze the T cell repertoire (Fig. 5 D; van Dongen et al., 2003; van Krieken et al., 2007). PCR products amplified from lymphocytes co-cultured with ADV-TT–infected UVECs showed a specific clonal expansion of TCRγ, as defined by an enhanced 220-bp single PCR band. This TCRγ clonal expansion against ADV-TT was completely inhibited by ADV–Tim-3 (Fig. 5 D), implying that the antigen-specific T cell response against ADV-TT was abolished by Tim-3. To address whether the responding subset of T cells were γδT cells, we repeated the Biomed-2 multiplex TCR PCR experiments using purified $CD4^+$ and $CD8^+$ cells co-cultured with ADV-TT–infected UVECs. A specific clonal expansion was detected both in $CD4^+$ and $CD8^+$ T cells, indicating that the responding clonal expansion to ADV-TT is via $CD4^+/CD8^+$ T cells rather than γδT cells. Again, the $CD4^+$ T cell clonal expansion was abolished by Tim-3–expressing ECs (Fig. 5 E).

We then asked whether the suppression of T cell proliferation by Tim-3 resulted in protective immunity (Fig. 5 F). Although autologous T lymphocytes activated by ADV-TT–infected dendritic cells effectively killed ADV-TT–infected UVECs, the killing efficacy was significantly inhibited by ADV–Tim-3 but not by ADV-GFP. To identify which T cell subsets were influenced by Tim-3, we observed the various T cell subsets in the presence or absence of ADV–Tim-3 (Table S1). Autologous T lymphocytes responded to ADV-TT–infected UVECs with significant proliferation. However, the proliferation of $CD4^+$ and $CD8^+$ T cells was significantly inhibited by ADV–Tim-3. Importantly, the $CD4^+/CD28^{high}$ T lymphocytes decreased significantly after exposure to ADV–Tim-3. On the other hand, the $CD8^+/CD28^{high}$ and T reg ($CD4^+/CD25^+/CD127^{low}$) cell populations (Tiemessen et al., 2007) were not altered by ADV–Tim-3 (Fig. 5 G). These data indicated that the immune target cells of Tim-3 were $CD4^+$, $CD4^+/CD28^{high}$ rather than the $CD8^+/CD28^{high}$ and T reg cell subsets, which is in agreement with our clinical data (Fig. 3, D and E).

We further identified that ADV–Tim-3 suppressed activation of $CD4^+/IFN\text{-}\gamma^+$ but not $CD8^+/IFN\text{-}\gamma^+$ (Fig. 5 H). To further confirm this finding, UVEC/T cell co-cultured supernatants were analyzed for the production of Th1/Th2 cytokines. Despite the fact that the production of IL-4 and IL-2 was not influenced by Tim-3, ADV–Tim-3 appeared to promote production of Th2 cytokines (IL-10; ADV–Tim-3 vs. ADV-GFP, $P = 0.005$) and inhibit the production of Th1 cytokines (IFN-γ and TNF; ADV–Tim-3 vs. ADV-GFP; Fig. 5 I). To further test whether Tim-3–expressing ECs derived from primary lymphoma tissues suppressed antigen-induced activation of $CD4^+$ T cells, a 15-mer peptide mapping to the 167–181 region of VEGFR-2 (which has been shown to induce a specific $CD4^+$ T cell response in several HLA-DR alleles [Sun et al., 2008], including DR4 and DR7) was used. ECs were purified from fresh lymph node tissues of lymphoma patients with HLA-DRB1*1501 ($n = 2$) and HLA-DRB1*0701 ($n = 1$), and the purity of the ECs was confirmed (Fig. S3 A). Notably, all of the ECs derived from the three lymphoma patients had negative expression of Tim-3 (Fig. S3 A). It should be emphasized that the ECs in this experiment were different from those used in other parts of the study. To obtain enough ECs for the present experiment, lymphoma ECs were isolated and amplified through a culture procedure taking >15 d. It is possible that ECs clonally related to lymphoma are not maintained or expanded under in vitro conditions, which is in agreement with our previous observations (Wu et al., 2009). Although the VEGFR-2 peptide–loaded ECs activated the autologous $CD4^+$ and $CD8^+$ T cell response, the $CD4^+$ activation was abolished by the expression of Tim-3 (Table S2). On the other hand, the $CD8^+$ was not altered by ADV–Tim-3, which led to a significantly decreased CD4/CD8 ratio (1.16 ± 0.22 vs. 2.37 ± 0.29; $P = 0.004$; Fig. S3 B).

To explore the possible mechanisms underlying the negative effects of Tim-3–expressing ECs on the activation of lymphocytes, UVECs infected with ADV-TT and ADV–Tim-3 were fixed with paraformaldehyde, incubated with CFSE-labeled lymphocytes, and subjected to proliferation assays. Although ADV-TT–stimulated lymphocyte proliferation was suppressed by Tim-3–expressing ECs, the suppression was partially reversed providing that Tim-3–expressing ECs were prefixed with paraformaldehyde (Fig. 6 A). These results imply that both the direct cell contact of ECs with lymphocytes and other factors may play roles in the suppression of lymphocyte activation. Next, we examined the effects

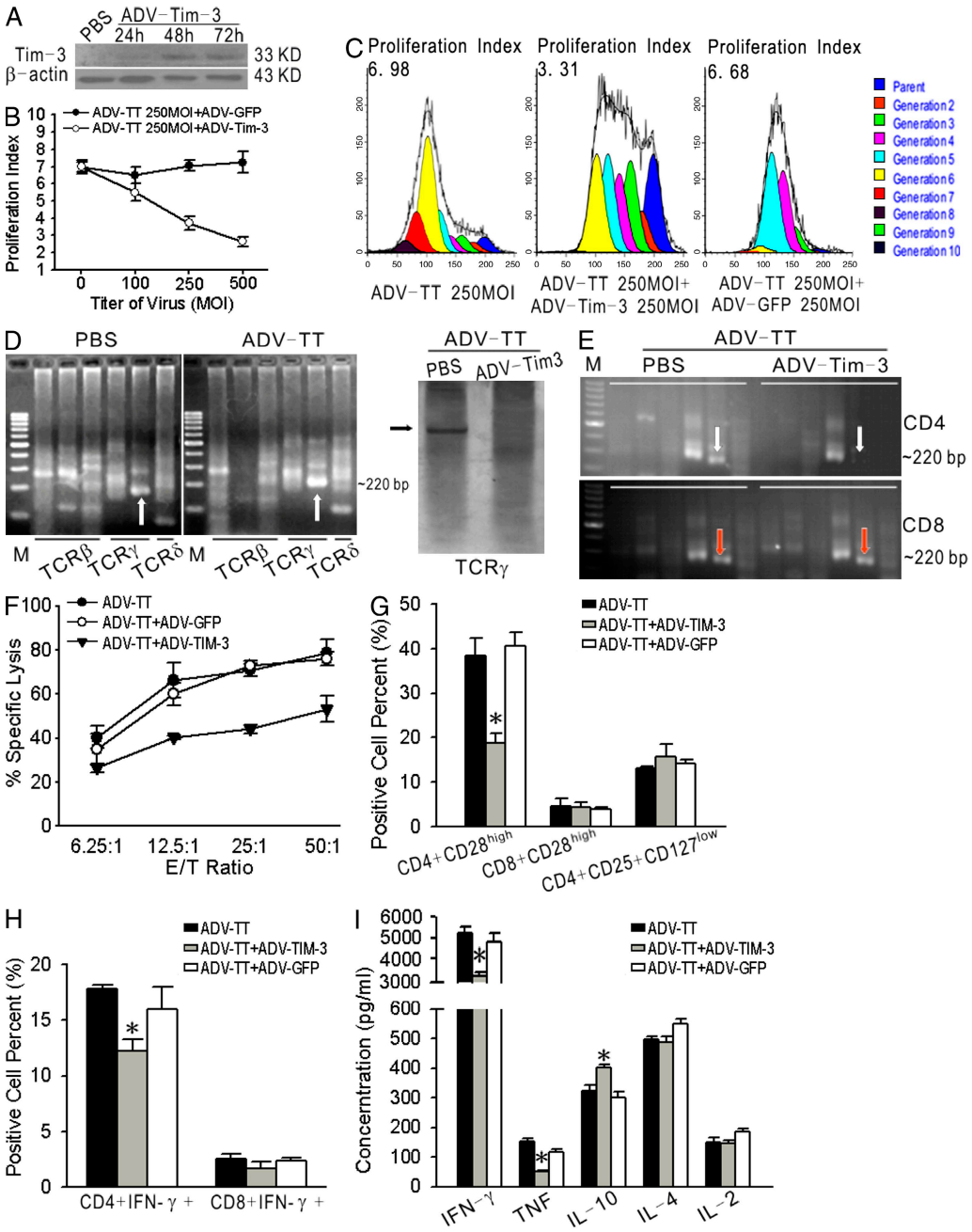

Figure 5. Expression of Tim-3 in UVECs abolished the activation of CD4⁺ T cells and provided protective immunity. (A) Expression of Tim-3 was determined by Western blotting in UVECs infected with ADV–Tim-3 or treated with PBS. (B) UVECs infected with various adenoviral mutants were incubated with CFSE-labeled lymphocytes and subjected to proliferation analysis. ADV–Tim-3 but not ADV-GFP inhibited the proliferation of lymphocytes. Data are represented as means ± SD of triplicates. (C) Typical CFSE profiles of lymphocytes with different treatments. (D) Biomed-2 multiplex TCR PCR to analyze the T cell repertoire after various treatments. UVECs infected with ADV-TT were incubated with lymphocytes. Multiplex PCR was used to amplify six TCR subfamily genes from activated lymphocytes. (left) A positive clonal TCRγ rearrangement against ADV-TT (arrows). (right) The positive clonal TCRγ rearrangement against ADV-TT (arrow) was inhibited by ADV–Tim-3. (E) Biomed-2 multiplex TCR PCR to analyze the T cell repertoire after various treatments. UVECs infected with ADV-TT were incubated with isolated CD4⁺ or CD8⁺ T cells. Multiplex PCR was used to amplify six TCR subfamily genes from activated lymphocytes. The positive clonal TCRγ rearrangement against ADV-TT was inhibited by ADV–Tim-3 in CD4⁺ T cells (white arrows) but not in CD8⁺ T cells (red arrows). (F) Lymphocytes were incubated with ADV-TT–infected dendritic cells. The resulting CTLs were added to ADV-TT–infected UVECs in the presence or absence of ADV–Tim-3. The culture supernatant was then determined by an LDH release assay for specific lysis. Data are represented as means ± SD of triplicates. (G) UVECs were infected with varied viral mutants and incubated with autologous lymphocytes. Lymphocytes were analyzed for T cell subpopulations. Data are represented as means ± SD of triplicates. (H) Lymphocytes were treated as described in G and analyzed for CD4⁺/IFN-γ⁺ and CD8⁺/IFN-γ⁺ populations. Data are represented as means ± SD of triplicates. (I) UVEC/T cell culture supernatants were measured for production of the Th1/Th2 cytokines IFN-γ, TNF, IL-10, IL-4, and IL-2. Data are represented as means ± SD of triplicates. Similar results were observed in three (A, B, and F–I) or four (D and E) independent experiments. *, $P < 0.01$.

of Tim-3 expression on the production of various cytokines in ECs. Strikingly, although the production of most of cytokines in ECs remained unaffected, Tim-3 expression increased the EC-derived production of IL-6 by almost 10-fold ($P < 0.01$; Fig. 6 B). To address the functional significance of increased IL-6 production in ECs, we initially examined the impact of recombinant IL-6 on the phosphorylation of the STAT3 protein in UVECs and ADV-TT–stimulated lymphocyte proliferation. We found that addition of IL-6 significantly increased the level of phosphorylated STAT3 (p-STAT3) in UVECs (Fig. 6 C). Furthermore, ADV-TT–stimulated lymphocyte proliferation was substantially inhibited by IL-6 (Fig. 6 D). To further confirm the critical role of p-STAT3 in Tim-3$^+$ EC–mediating immunosuppression, we examined the level of p-STAT3 in Tim-3–expressing UVECs. As expected, STAT3 phosphorylation was strikingly enhanced in Tim-3–expressing UVECs (Fig. 6 E). Interestingly, S3I201, a specific STAT3 inhibitor, inhibited the phosphorylation of STAT3 and consequently abolished the immunosuppressive effects of Tim-3–expressing ECs ($P < 0.05$; Fig. 6 F). Obviously, the effect of S3I201 is not caused by nonspecific effects, because S3I201 at a dose of 50 μM did not increase apoptosis of UVECs or alter the expression of MHC and co-stimulatory molecules in UVECs (unpublished data). To explore the effects of engagement of Tim-3 by its ligands (e.g., galectin-9), Tim-3–expressing UVECs were analyzed for production of IL-6 in the presence of recombinant galectin-9 protein. Strikingly, galectin-9 substantially enhanced the secretion of IL-6 in Tim-3–expressing ECs (Fig. 6 G). To explore the interaction between Tim-3 and T lymphocytes, we incubated autologous CD4$^+$ or CD8$^+$ lymphocytes with a DsRed recombinant Tim-3 fusion protein to identify the target T subsets. Our results revealed that CD4$^+$ ($7.12 \pm 0.55\%$) but not CD8$^+$ ($0.25 \pm 0.18\%$) T cells were the target cells bound by DsRed Tim-3 (Fig. 6 H). Consistent with our data observed with recombinant galectin-9, Tim-3–expressing ECs in the presence of paraformaldehyde-fixed CD4$^+$ T cells increased IL-6 secretion by almost 30-fold and substantially promoted the phosphorylation of STAT3 in UVECs ($P < 0.01$; Fig. 6, I and J). These data argue for a critical role of the interaction between CD4$^+$ T cells and Tim-3–expressing ECs in suppressing lymphocyte activation through activation of the IL-6–STAT3 pathway. To support this notion, our protective immunity assay showed that the immunoprotection mediated by Tim-3 was considerably diminished by an anti-CD4 antibody (Fig. 6 K).

Tim-3–expressing ECs facilitate the progression of lymphoma in vivo

We next determined whether Tim-3–expressing ECs facilitated the progression of lymphoma in a mouse model, and the characterization of lymphoma in TA2 mice was confirmed (Fig. S4, A–E). The TA2 mice lymphoma was a B-lineage lymphoma. To observe the effects of Tim-3–expressing ECs on the growth of lymphoma in vivo, ECs were isolated from the bone marrow of healthy TA2 mice and infected with ADV-GFP or ADV–Tim-3 before injection into the same site for lymphoma inoculation. The presence of adenoviral mutant–infected ECs in vivo was confirmed by tracking ADV-GFP. 1 d after the EC injection, the engrafted ECs scattered within the tumor (Fig. S4 F). 2 d after the injection, some microvessels formed by the engrafted ECs were detected (Fig. S4 G). Importantly, Tim-3–expressing ECs significantly accelerated the onset of lymphoma when compared with ADV-GFP– or PBS-treated ECs (Fig. 7, A and B). More importantly, all mice that received ADV–Tim-3–infected ECs displayed evidence of dissemination within 26 d of inoculation. In the same experiments, only 25% of the mice in the PBS control group and 12.5% of the mice in the ADV-GFP group were found to have disseminated tumors. The CD4$^+$ T lymphocytes in peripheral blood collected from lymphoma-bearing mice from all three groups were analyzed 26 d after inoculation with lymphoma cells (Fig. 7 C). The percentage of CD4$^+$ T lymphocytes from PBS- or ADV-GFP–treated mice was significantly higher than that of ADV–Tim-3–treated mice (ADV–Tim-3 vs. PBS group, $P = 0.004$; ADV–Tim-3 vs. ADV-GFP group, $P = 0.02$). The CD4$^+$ lymphocytes in the spleens of ADV–Tim-3–treated mice also showed a decrease when compared with those from control mice treated with PBS or ADV-GFP (ADV–Tim-3 vs. PBS group, $P = 0.017$; ADV–Tim-3 vs. ADV-GFP group, $P = 0.033$; Fig. 7 D). In the same experiment, CD8$^+$ lymphocytes exhibited a decreasing trend in the ADV–Tim-3–treated group, but no statistically significant difference was observed. We next analyzed the serum, spleen cells, and lymphoma tissue for basal levels of Th1 (IFN-γ, TNF, and IL-2) and Th2 (IL-5 and IL-4) cytokines. In the ADV–Tim-3 group, the basal levels of Th1 cytokines (TNF in serum, TNF and IFN-γ in spleen cells and lymphoma tissue) were significantly lower than those in the ADV-GFP or PBS group (Table S3). We further analyzed the lymphocytes that infiltrated the tumor and found that the CD4$^+$ T cell subset was significantly lower in the ADV–Tim-3 group (ADV–Tim-3 vs. PBS group, $P = 0.025$; ADV–Tim-3 vs. ADV-GFP group, $P = 0.01$; Fig. 7 E), although no significant change was observed in CD8$^+$ T cell numbers (Fig. 7 F). To test whether Tim-3–expressing ECs facilitated the development of lymphoma via inhibition of CD4$^+$ T cells, A20 mice B cell lymphoma models were used. Anti-CD4 blocking antibody significantly accelerated the onset of lymphoma compared with the PBS-treated group (Fig. S5 A). More importantly, Tim-3–expressing ECs did not further accelerate the onset of lymphoma in mice models pretreated with anti-CD4 blocking antibody, implying that the immunosuppressive effects of Tim-3–expressing ECs act through inhibition of CD4$^+$ T cells. To further support this notion, we examined whether injection of Tim-3–expressing ECs inhibited the activation of T cell responses against the delayed type hypersensitivity (DTH) response. Again, Tim-3–expressing ECs significantly diminished the DTH response as defined by ear swelling ($P < 0.05$; Fig. S5, B–D) and spleen edema reactions ($P < 0.05$; Fig. S5 E).

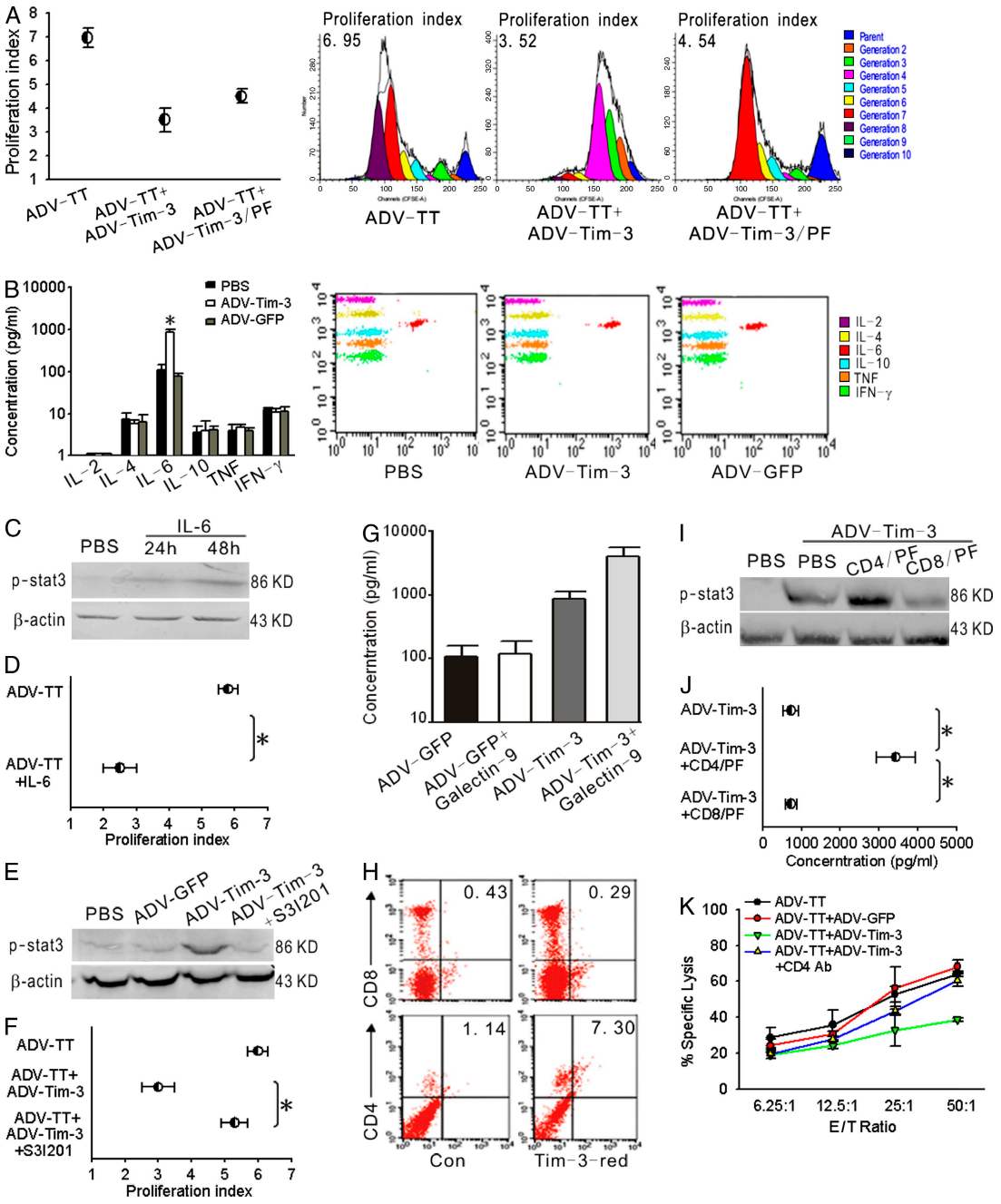

Figure 6. Mechanisms underlying the negative impact of Tim-3–expressing ECs on the activation of lymphocytes. (A) UVECs infected with ADV-TT and ADV–Tim-3 were fixed with 2% paraformaldehyde, incubated with CFSE-labeled lymphocytes, and subjected to proliferation analysis. (left) Although ADV-TT–stimulated lymphocyte proliferation was suppressed by Tim-3–expressing ECs, the suppression was partially reversed if Tim-3–expressing ECs were fixed by paraformaldehyde. (right) Typical CFSE profiles of lymphocytes in response to different treatments. PF, UVECs fixed with 2% paraformaldehyde. (B) The supernatants of UVECs infected with various adenoviral mutants were determined for production of the Th1/Th2 cytokines IL-2 (purple), IL-4 (yellow), IL-6 (red), IL-10 (blue), TNF (orange), and IFN-γ (green). Data are represented as means ± SD of triplicates. (right) Typical results of CBA analysis determined by flow cytometry. (C) UVECs were treated with 50 ng/ml IL-6 or PBS (negative control) for 48 h and analyzed for levels of p-STAT3. (D) UVECs were treated as described in C and subjected to lymphocyte proliferation analysis. (E) UVECs were treated as depicted and examined for levels of p-STAT3 protein. S3I201, UVECs treated with 50 µM S3I201 for 48 h. (F) UVECs were treated as described in E, and lymphocyte proliferation index were determined. (G) 300 µl of supernatants containing recombinant galectin-9 was mixed with 200 µl of culture medium, added into UVECs infected with ADV-GFP or ADV–Tim-3, and cultured for 48 h before IL-6 assays. Supernatants from empty vector-transfected CHO cells were used as a control. (H) 200 µl of CHO cell supernatants (from cells transfected with pTim-3–RED [right] or pDsRed-Express-1 [left]) was added to 5×10^5 autologous T lymphocytes. After incubation for 3 h, the cells were subjected to flow cytometry analysis for the percentage of RED-positive cells. Con, addition of supernatant of the CHO cells transfected with pDsRed-Express-1 (left). (I) Tim-3–expressing UVECs were incubated with paraformaldehyde-fixed

DISCUSSION

Although Tim-3–expressing $CD4^+$ T cells have previously been shown to interact with the Tim-3 ligand, inhibit effector Th1 cells during the normal immune response, and induce peripheral tolerance (Kuchroo et al., 2003; Sabatos et al., 2003; Sánchez-Fueyo et al., 2003; Zhu et al., 2005), their role in inducing tumor immune evasion has not been recognized. The present findings highlight a novel molecular mechanism by which expression of Tim-3 in the lymphoma endothelium causes active interaction with circulating T cells, suppresses the activation of $CD4^+$ T cells, and contributes to the establishment of lymphoma immune tolerance. Because the essential role of $CD4^+$ T cells in antitumoral immunity is well established, suppression of the activation of the $CD4^+$ T cell response by the tumoral endothelium is intriguing. The present findings strongly support a critical role for endothelial tissue in lymphoma progression, and suggest that the lymphoma endothelium is not only a vessel system that supplies oxygen and nutrients to tumor sites but also a functional barrier that assists the tumor in immune evasion (Gunsilius et al., 2000; Fidler and Ellis, 2004; Rigolin et al., 2006; Pezzolo et al., 2007; Gao et al., 2008). Recently, an independent group has shown that survival of DLBCLs after treatment was substantially influenced by the gene expression signatures of certain types of tumor microenvironments. DLBCLs with the signature that reflected increased lymphoma blood vessel density were associated with adverse clinical outcome (Lenz et al., 2008). These findings are very consistent with our data and strongly support our conclusions.

Previous well-known mechanisms of immune evasion by tumors involve several factors, such as tumor cells, T reg cells, dendritic cells, and mesenchymal stem cells (Kim et al., 2006; Karnoub et al., 2007). The findings presented here should extend our understanding of tumor immune evasion by underscoring the critical role of lymphoma-derived ECs. That the lymphoma endothelium works as an immune barrier that actively suppresses antitumoral immunity is a novel and important concept for the following reasons. First, human endothelial tissue is composed of $1–6 \times 10^{13}$ ECs lining a total surface area of 4,000–7,000 m^2, and they form an enormous interface between circulating immune cells and underlying tissues (Danese et al., 2007). Second, a significant proportion of lymphoma-derived ECs have lymphoma-specific chromosomal translocations, which give rise to lymphoma-specific antigens (Streubel et al., 2004). In addition, a dominant proportion of circulating ECs in bone marrow or peripheral blood also harbors tumor-specific chromosomal translocations in some malignancies (Wu et al., 2009), and can potentially interact with the immune system. Third, mounting evidence supports the notion that ECs act as semiprofessional APCs and present antigens to T cells as an immune surveillance mechanism (Choi et al., 2004; Danese et al., 2007). Although professional APCs induce antitumoral immunity, in our hands, lymphoma-derived ECs expressed lymphoma antigens and then induced immune tolerance to the antigens by expressing Tim-3. It appears that Tim-3–expressing ECs inhibit the response of lymphocytes to antigens through the activation of the STAT3 pathway. Tim-3 expression considerably enhanced EC-secreted IL-6, gave rise to an elevated level of p-STAT3, and suppressed the activation of lymphocytes. Furthermore, the cascade of IL-6 production and consequent STAT3 phosphorylation was substantially enhanced by an interaction of Tim-3–expressing ECs with $CD4^+$ cells, the target T subset for Tim-3. Currently, there are several important questions that remain to be addressed. For example, what is the exact subpopulation of $CD4^+$ T cells bound by EC-associated Tim-3? What is the exact receptor on the $CD4^+$ cell surface for binding Tim-3–expressing ECs? What are the functional fates of $CD4^+$ T cells upon binding to Tim-3–expressing ECs? The answers to these questions will clarify the question of why $CD8^+$ T cells were less affected by Tim-3–expressing ECs and extend our understanding of the mechanisms underlying tumor evasion and improve the targeting of future therapies. Nevertheless, our results suggest that angiogenesis is far more crucial to lymphoma progression than was previously thought. Not only does the lymphoma endothelium facilitate the successful dissemination and progression of lymphoma by supplying oxygen and metabolites and allowing lymphoma cells to access the vasculature and spread to distal sites, but it also switches off immune surveillance. Thus, acquisition of increased potential for lymphoma dissemination could be endowed and maintained by lymphoma ECs by themselves.

Our findings have important clinical implications. Lymphoma is considered to be a potentially curable malignancy; however, a large number of cases of advanced lymphoma eventually become refractory or relapse after initial treatment because of the persistence of residual disease. These patients are considered incurable using the available treatment options, and there is an urgent need for novel treatment modalities. Active immunotherapy is a promising approach and is being investigated as a next generation strategy for lymphoma treatment. Current immune therapy includes several approaches, such as idiotype vaccines, DNA vaccines, and engineering antigen-specific T cells (Maloney, 2005). Whatever the active immunotherapy approach used, the penetration of activated T cells through the lymphoma endothelium is one of the most important factors for determining antitumoral efficacy. The

$CD4^+$ or $CD8^+$ T cells and the levels of p-STAT3 were determined. (J) Tim-3–expressing UVECs were treated as described in I and the production of IL-6 was determined. (K) Lymphocytes were incubated with ADV-TT–infected dendritic cells. The resulting CTLs were added to ADV-TT–infected UVECs in the presence or absence of ADV–Tim-3. Anti-CD4 blocking antibody was added into the co-cultured system at a final concentration of 8 µg/ml. The culture supernatant was then examined by an LDH release assay for specific lysis. Data are represented as means ± SD of triplicates. Similar results were observed in four (A and C–F) or three (B and G–K) independent experiments. *, $P < 0.05$.

lymphoma endothelium–mediated immune suppression of the CD4$^+$ T cell response further proves that it is necessary to therapeutically target immune suppression mechanisms in addition to using adoptive immune therapy. Finally, there is mounting evidence for the critical role of the tumor microenvironment in tumor dissemination (Karnoub et al., 2007; Steeg and Theodorescu, 2008). If the increased metastatic potential of tumor cells can be initiated and maintained by the

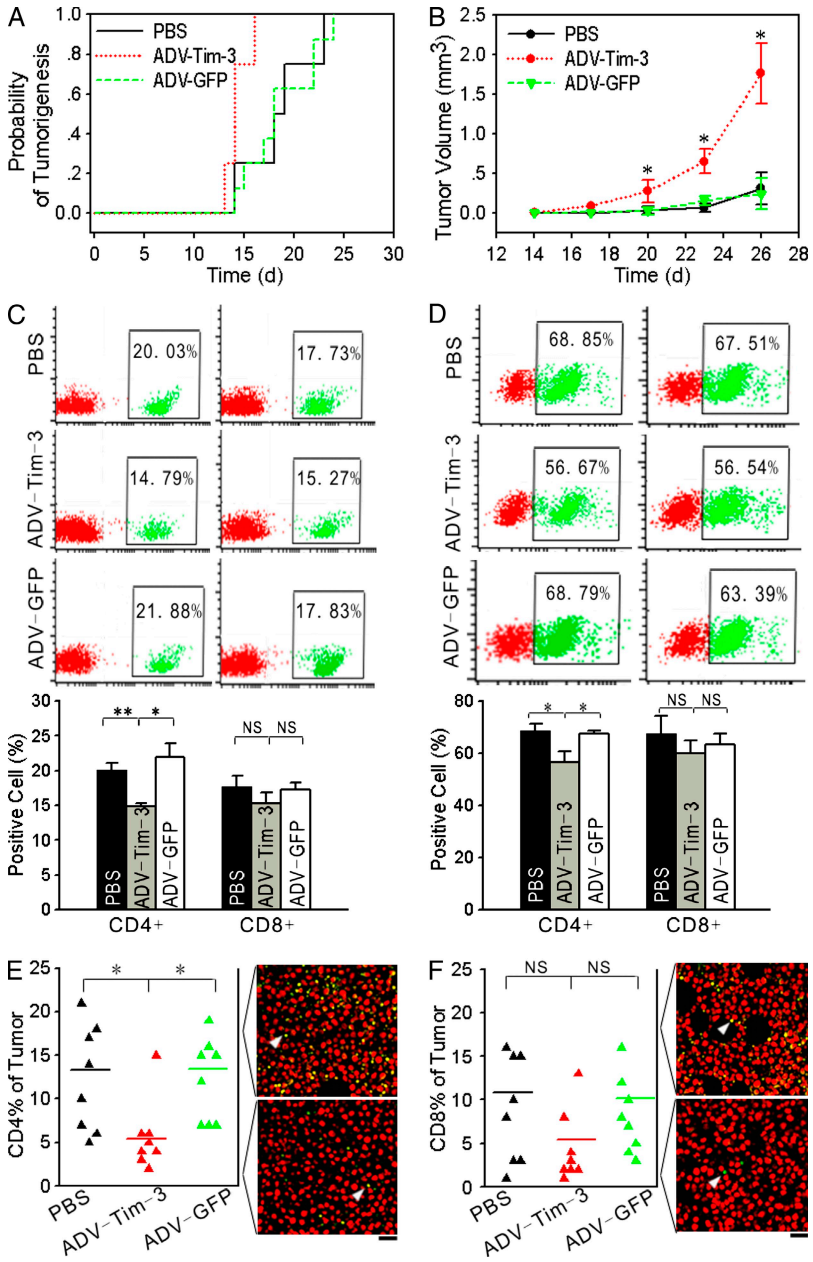

Figure 7. Tim-3–expressing ECs impair T cell antitumor immunity and facilitate tumor growth in vivo. TA2 mice were inoculated into the inguinal groove muscle with 5 × 10^5 lymphoma cells. ECs were isolated and purified from the bone marrow of healthy TA2 mice and infected with ADV-Tim-3, ADV-GFP, or PBS. Each group included eight model mice. 5 × 10^4 ECs were injected into the same site for tumor inoculation on days 3, 6, and 9 after tumor implantation. (A) Cumulative probability of tumor onset was determined by the appearance of neoplasms into the inguinal groove muscle. In PBS- or Adv-GFP–treated EC groups, lymphoma formation at the inoculation sites took an average of 18.5 ± 3.4 d or 18.8 ± 3.6 d, respectively, whereas ADV–Tim-3–infected ECs significantly shortened the formation time of lymphomas at primary sites to 14.3 ± 1.2 d (ADV–Tim-3 versus PBS group, P = 0.01; ADV–Tim-3 versus ADV-GFP group, P = 0.01). (B) Tumor volume was monitored. (C) Peripheral blood cells and (D) spleen cells from TA2 mice were stained with an FITC-conjugated mAb to mouse CD4 and CD8 and analyzed by flow cytometry. (top) Representative data of flow cytometry analysis. (bottom) Data in columns are representative of four experiments and represented as means ± SD. (E) CD4$^+$ and (F) CD8$^+$ T cell populations as percentages of total tumor cells are shown. Horizontal bars represent means. Representative immunofluorescence images of infiltrating lymphocyte populations (green; arrowheads) are shown against the background of tumor cells (red). Bars, 20 µm. *, P < 0.05; **, P < 0.01.

tumor-derived endothelium, targeting lymphoma angiogenesis is expected to curtail and possibly even reverse lymphoma dissemination. Further evaluating the contribution of the endothelium in immune evasion of lymphoma and other solid tumors will provide novel strategies for controlling tumor dissemination by targeting tumor-derived ECs.

MATERIALS AND METHODS

Tissue samples. Lymph node samples were obtained at the time of surgery for diagnostic purposes according to a protocol approved by the Institutional Review Board for Human Research at Tongji Hospital. Lymph nodes were collected from 134 patients: 30 cases with DLBCL, 22 cases with peripheral T cell lymphoma, 53 cases with other types of lymphoma, and 29 cases with reactive lymph nodes. No chemotherapy or radiotherapy was performed before collection of the tissue samples. All samples were sectioned for both immunohistochemical and hematoxylin and eosin staining for histological diagnosis by pathologists according to the classification of the World Health Organization. For GeneChip probe arrays and validation of microarray data, a higher quality tissue free of RNA degradation was needed. Samples for this purpose were therefore collected separately and processed according to our previous description (Bai et al., 2008). An additional 53 lymph node samples were obtained, of which 13 were used for microarray analysis, 20 were used for in situ hybridization, and 12 were used for purification of ECs for cell culture. Eight lymph nodes were not used because of the poor sample quality or being diagnosed as metastatic cancer.

Oligonucleotide microarray for endothelium isolated from lymph node tissues. Endothelium was isolated from primary lymph node tissues and subjected to RNA microarray analysis for global gene expression profiles according to our previously published protocol (Neri and Bicknell, 2005). In brief, lymph nodes were obtained within 15 min after removal from the patients. Under RNase-free conditions, lymph nodes were retrieved and immediately immersed in prechilled fixatives. The sections of the samples were evaluated by pathologists for histological diagnosis and subjected to immunohistochemical staining with an anti-CD34 antibody to mark endothelium in the frozen sections. The endothelium (equal to ~6,000 ECs) was isolated using LCM and subjected to RNA extraction. Half of the isolated RNA was used for the quality control of the LCM-captured endothelium. To examine the purity of the isolated endothelium and possible contamination by nonendothelium tissues, RT-PCR was performed to amplify transcripts of CD34, CD19, CD20, and CD3. To amplify a 213-bp CD19 fragment, a sense primer (5′-CAGCTGACCTGGTCTCGGGAGT-3′) and an antisense primer (5′-CCCGCTGCCCTCCACATTGACT-3′) were used. To amplify a 223-bp CD34 fragment, a sense primer (5′-GTGGCTGATACCGAATTGTGAC-3′) and an antisense primer (5′-CTCCAGGGAGCGAATGTGTAAA-3′) were used. To amplify a 242-bp human CD20 fragment, a sense primer (5′-TACACCTGCCTCATGCTCAG-3′) and an antisense primer (5′-TTCACAAGCCTTCTCACACG-3′) were used. To amplify a 223-bp CD3 fragment, a sense primer (5′-TGAGGGCAAGAGTGTGTGAG-3′) and an antisense primer (5′-TAGTCTGGGTTGGGAACAGG-3′) were used. To amplify a 180-bp β-actin internal control fragment, a 5′ sense primer (5′-CTCACGAAACTGGAATAAGC-3′) and a 3′ antisense primer (5′-AAGCCACACGTACTAAAGGT-3′) were used. If contamination of nonendothelium tissues was excluded, which was defined as no amplification of transcripts of lymphocyte markers (CD19, CD20, or CD3), the samples were used for subsequent GeneChip probe arrays. Total RNA was extracted, underwent a nonbiased nucleic acid amplification procedure, and was subsequently subjected to oligonucleotide microarray analysis. A GeneChip Human Genome U133 Plus 2.0 Array (Affymetrix) was used for the current study. This array comprises 1,300,000 unique oligonucleotide probes covering >47,000 transcripts and variants, which represents ~39,000 of the best-characterized human genes. A probe set consists of 11–20 probe pairs for detecting each expressed transcript. The analysis software that accompanied the microarray (Suite 5; Affymetrix) was used to process the data from the GeneChips. This software allowed us to calculate the signal and determine whether an expressed transcript was present or absent. Microarray data have been deposited in the Gene Expression Omnibus under accession no. GSE19882.

In situ hybridization. In situ hybridization was performed on lymph node tissue cryosections with 1 μg/ml of biotinylated oligonucleotide probe complementary to the Tim-3 coding region (5′-TGCTGCTACTACTTACAAGGTCCTCAGAAGTGGAATACAGAGCGGAGGTC-3′). Negative controls were similarly processed with the probe omitted.

Immunohistochemistry. Paraffin-embedded tissue sections were dewaxed in xylene and subjected to immunohistochemical analysis as previously described (Geng et al., 2006). An anti-CD34 mouse monoclonal antibody (Changdao Biotech Co.), anti–Tim-3 goat polyclonal antibody (Santa Cruz Biotechnology, Inc.), and biotinylated secondary antibody were used in the present study. For semiquantitative evaluation, an immunoreactivity-scoring (IRS) system was applied. Intensity of staining was designated as either nonexistent (0), weak (1), moderate (2), or strong (3). The percentage of positive cells was termed as the expression score. The IRS was calculated by multiplying the expression score with the intensity score and ranged from 0–3. Samples with IRS scores of 0–1 point were considered negative for Tim-3 expression; otherwise, the samples were designated as positive. These data were analyzed along a continuum, and the objective was to use this semiquantitative method to assess differences between various experimental groups. For analysis of MVD, the microvessels were labeled with anti-CD34 antibody and counted under a low-power field (200×). MVD counts were defined as the number of microvessels per 0.2 mm^2. Criteria for positive staining and microvessel counting followed the method described by Weidner (1995). The mean MVD values were calculated in five areas of the tumors. For characterization of lymphoma immune profiles, 24 cases of DLBCL were divided into two groups according to positive (n = 12) or negative (n = 12) expression of Tim-3 in the microvascular endothelium. Primary antibodies included anti-CD4, anti-CD8, and anti-CD1a (all from Dako). A horseradish peroxidase kit (EnVision+ System; Dako) was used to detect immune reactivity. The slides were read and scored by two pathologists who blinded each other to prevent observer bias. Data resulting from cell counts and area represent an average of five high-power fields (Coventry and Morton, 2003). Each data point represents the mean of the results from two pathologists.

Preparation of cells. Purification of ECs from fresh lymph nodes were performed as described previously (Streubel et al., 2004). The purified ECs were then processed for other experiments. For isolation of UVECs, umbilical cords provided by healthy human volunteers were processed as described previously (Cooke et al., 1993) and cultured in M199 supplemented with 20% FCS, 10 ng/ml of epithelial growth factor, 35 μg/ml gentamycin, 1 μg/ml hydrocortisone, and 2.5 μg/ml amphotericin B. UVECs were digested using 0.25% trypsin and 1 mM EDTA (Invitrogen), seeded onto uncoated 24-well plates, and cultured for 4 d. Each experiment used first-passage cells from one umbilical cord. Autologous T lymphocytes were obtained from heparinized cord blood of the same volunteers according to a standard protocol using Ficoll-Hypaque (GE Healthcare) density-gradient centrifugation. To study the interaction of UVECs with autologous T cells, UVECs were infected with various adenoviral mutants at different titers. Autologous T lymphocytes were then mixed with the UVECs at a ratio of 10:1 in the presence of 50 U/ml IL-2 (Sigma-Aldrich) for the first round of vaccination. On day 4, T lymphocytes were transferred into a new well with infected UVECs for the second round of vaccination, lasting for another 3 d. Cord blood–derived dendritic cells were generated as described previously (Wong et al., 2005).

Adenoviral mutants. All adenoviral mutants used in the present study were constructed in our laboratory following standard protocols described previously (Zhou et al., 2005). ADV-GFP contains a GFP gene under the control of a Rous sarcoma virus long terminal repeat promoter in the region of the excised E1 adenoviral genes. All other replication-deficient adenovirus

vectors used in this study were constructed using the AdEasy system (MP Biomedicals) according to the manufacturer's instructions. The ADV-TT expression cassette contains an exogenic gene of TT, which is composed of parts of fragment C of TT (aa 865–1120 and 1162–1169 of TT), with a leader sequence derived from the H chain variable region of the IgM of a B cell lymphoma.

Flow cytometry. A FACScan cytometer and CellQuest software (both from BD) were used for data acquisition and analysis. To determine the purity of ECs isolated from lymph nodes, the cells were double stained with directly conjugated anti-CD31 (FITC; BD) and anti-CD105 (PE; BD). To determine the expression of MHC and co-stimulatory molecules, cultured UVECs were stained with either directly conjugated anti–MHC class I (FITC; BD), anti–MHC class II (FITC; BD), anti-CD80 (FITC; BioLegend), or anti-CD58 (PE; BioLegend). To study the interaction of UVECs with autologous T cells and the effects of Tim-3 on this interaction, umbilical vein T lymphocytes were stimulated by autologous UVECs infected with different adenoviral mutants. The cells were then stained with directly conjugated anti-CD4, anti-CD8, anti-CD28, anti-CD25, anti-CD127, or anti–IFN-γ (BD). To determine the influence of various adenoviral mutants on the survival of UVECs, UVECs were infected with various adenoviral mutants for 72 h and resuspended in binding buffer. 5 μm FITC plus annexin V (BD) and 10 μl propidium iodide solution at a concentration of 50 μg/ml in PBS were added, and the cells were incubated for 20 min at room temperature in the dark. Stained cells were then subjected to flow cytometry analysis.

RT-PCR. To detect isoforms of Tim-3 transcripts, RT-PCR was performed. Total RNA was extracted from freshly isolated lymphoma ECs. A 5′ sense primer (5′-CGGAGGTCGGTCAGAATGCCTATC-3′) and a 3′ antisense primer (5′-GGGCTCCTCCACTTCATATACGTTC-3′) were used to amplify Tim-3 transcripts. The expected product for full-length Tim-3 is 749 bp and for sTim-3 is 541 bp. A 5′ sense primer (5′-CTCACGAAACTG-GAATAAGC-3′) and a 3′ antisense primer (5′-AAGCCACACGTACTA-AAGGT-3′) were used to amplify a 180-bp β-actin internal control.

Western blotting. Preparation of protein samples and Western blots were performed as described previously (Gao et al., 2006).

Cell proliferation assays. Lymphocyte proliferation assays were performed as previously described (Coupel et al., 2004). In brief, after erythrocyte lysis, 3–4 × 10^7 cells were suspended in 500 μl RPMI 1640, and 4 μl of a solution prepared by mixing 50 μl of 5 mM CFSE (Sigma-Aldrich) stock solution and 450 μl DMSO (AppliChem) was added. The cell solution was then incubated for 30 min at 37°C and washed twice with 10 ml PBS (+0.1% BSA) afterward. The cells were resuspended in 500 μl of 0.9% NaCl and again counted in a counting chamber. Lymphocytes were stimulated with UVECs infected with various adenoviral mutants after 3 d and again 3 d later. The staining was assayed by FACS analysis, and the proliferation index was processed with FlowJo software (Tree Star, Inc.). The proliferation index was defined as the sum of the cells in all generations divided by the calculated number of original parent cells. This was useful for comparing the quantity of all cell divisions among cultures of the same kinds of cells undergoing different treatments.

Biomed-2 multiplex TCR PCR. To assess clonal expansion of T lymphocytes in response to ECs infected with ADV-TT, the Biomed-2 multiplex TCR PCR technique was used, as described previously (van Dongen et al., 2003). In brief, multiplex PCR was used, according to a standardized Biomed-2 PCR protocol, to amplify six subfamily genes, including TCRβ, TCRγ, and TCRδ, of TCRs from activated lymphocytes. The PCR products were run on 1.5% agarose gels or 6% denatured polyacrylamide gels (SILVER SEQUENCE Staining Reagents; Promega) for heteroduplex analysis. A specific PCR band visible in the corresponding position was judged as a positive clonal TCR rearrangement (van Dongen et al., 2003). To address which subset of T cells was clonally expanded, $CD4^+$ and $CD8^+$ cells were isolated by magnetic cell sorting columns (MACS; Miltenyi Biotec). The Biomed-2 multiplex TCR PCR experiment was then repeated using purified $CD4^+$ and $CD8^+$ cells co-cultured with ADV-TT–infected UVECs.

Cytotoxicity assay. Dendritic cells were infected with ADV-TT at an MOI of 250 for 2 h and cultured for another 24 h. TT-loaded dendritic cells were harvested and added to a culture plate of autologous T lymphocytes at a ratio of 1:20 after 5 d and again 5 d later. The resulting lymphocytes were added to UVECs infected with various adenoviral mutants at different E/T ratios in triplicate for 4 h. The culture supernatant was determined by a standard lactate dehydrogenase (LDH) release assay using an LDH cytotoxicity assay kit (Biovision Inc.). Specific lysis was determined as follows: percentage of specific release = 100 × (experimental release − spontaneous release)/(maximum release − spontaneous release). For quality control, spontaneous release must be <20% of the maximum release in all experiments.

Cytokine bead assay (CBA). To measure cytokine levels, a CBA was performed using a CBA immunoassay kit (CBA Human Th1/Th2 Cytokine Kits I and II; BD) according to the manufacturer's instructions. Data were acquired using a flow cytometer (FACSCalibur; BD).

Fixation of cells. For fixation experiments, ECs were digested using 0.25% trypsin and 1 mM EDTA, seeded onto uncoated 24-well plates, infected with various adenoviral mutants at an MOI of 250 for 2 d, and fixed with 2% paraformaldehyde for 1 h at 4°C. Thereafter, fixed cells, together with the untreated fraction, were washed extensively and mixed with CFSE-labeled autologous T lymphocytes for proliferation assays. For fixation of $CD4^+$ and $CD8^+$ T cells, the cells were isolated and fixed with 2% paraformaldehyde for 1 h at 4°C before co-culturing with ECs for cytokine assays.

Preparation of recombinant protein. An expression plasmid of human recombinant galectin-9 protein was constructed as described previously (Nobumoto et al., 2008). Chinese hamster ovary (CHO) cells were transfected with the plasmid indicated in the figures with Lipofectamine 2000 (Invitrogen) transfection reagent. The transfected cells were selected in complete medium containing 1 mg/ml G418 (Invitrogen) and were subsequently cloned by limiting dilution. The supernatants of the transfected cells were collected, the abundance of galectin-9 was detected by Western blotting, and the supernatants were then stored at −80°C for future experiments. To produce recombinant Tim-3 protein labeled with red florescent protein, a cDNA sequence encoding the signal peptide and extracellular domain of Tim-3 was synthesized by the AuGCT Biotechnology Corporation and inserted into the *Sac*I–*Apa*I site of a pDsRed-Express-1 vector to generate pTim-3–RED. The constructed pTim-3–RED was confirmed by DNA sequencing and expected to express a fusion protein consisting of the extracellular domain of Tim-3 with the RED fragment at its C terminus. CHO cells were transfected with pTim-3–RED or pDsRed-Express-1. The transfected cells were selected in complete medium containing 1 mg/ml G418 and subsequently cloned by limiting dilution. Expression of pTim-3–RED or pDsRed-Express-1 was examined by fluorescence microscopy. The supernatants of the transfected cells were collected, the abundance of Tim-3–RED was detected by Western blotting, and the supernatants were stored at −80°C for future experiments.

Mouse tumor model studies. All animal protocols were approved by the Institutional Animal Care and Use Committee of Tongji Medical College. Male and female TA2 mice were obtained from the Animal Experimental Center of Tianjin Cancer Institute. An experimental model of transplantable B lymphoma in TA2 mice was established. This model was derived from spontaneous lymphoma in a TA2 mouse, remained stable past 43 generations by successful transplantations in TA2 mice over 4 yr, and developed rapidly growing and highly invasive metastases in 100% of mice. Mice were randomized when 4–6 wk of age and inoculated with 5 × 10^5 lymphoma cells into the inguinal groove muscle. ECs were isolated and purified from the bone marrow of healthy TA2 mice as previously described (Göthert et al., 2004), and infected with ADV–Tim-3 (n = 8), Adv-GFP (n = 8), or PBS (n = 8) at an MOI of 500. 5 × 10^4 ECs were injected into the same sites 3, 6, and 9 d

after inoculation. The onset of the primary tumor was defined as a tumor diameter >0.2 cm^3, and lymphoma dissemination was defined as a remote lymph node diameter >0.2 cm^3. The growth and dissemination of lymphoma were monitored weekly until mice were sacrificed (26 d after inoculation). The peripheral blood, spleen, and primary lymphomas were obtained from model mice, stained with anti-CD4 and anti-CD8 (BD), and subjected to CBA to detect production of Th1/Th2 cytokines.

Statistical analysis. The SPSS statistical software program was used to test for correlations between quantitative variables by the establishment of nonparametric linear regression. The percentages of $CD4^+$ and $CD8^+$ T cell and $CD1a^+$ dendritic cell subsets were analyzed with the Mann-Whitney *U* test. Data are presented as means ± SD of at least three experiments and were analyzed by one-way analysis of variance followed by the Student-Newman-Keuls test. All p-values were two-sided, and $P < 0.05$ was considered significant. SPSS software (version 11.5) was used for all statistical procedures.

Online supplemental material. Table S1 shows the fluctuation of lymphocyte subsets in umbilical vein T lymphocytes after stimulation of autologous ECs infected with various adenoviral mutants. Table S2 shows the fluctuation of lymphocyte subsets in peripheral blood T lymphocytes after stimulation of autologous ECs infected with adenoviral mutants. Table S3 shows that Tim-3–expressing ECs inhibit basal levels of Th1 cytokines in vivo. Fig. S1 shows the levels of Tim-3 expression on endothelium in breast cancer and mastopathia tissues. Fig. S2 shows the possible correlation of $CD34^+Tim\text{-}3^+$ ECs with $CD4^+Tim\text{-}3^+$ T cells in lymphoma samples. Fig. S3 shows that Tim-3–expressing ECs derived from primary lymphoma tissues suppress antigen-induced activation of $CD4^+$ T cells. Fig. S4 shows the characterization of transplantable lymphoma in TA2 mice models. Fig. S5 shows the onset of lymphoma in mice models pretreated with anti-CD4 blocking antibody and the effects of Tim-3–expressing ECs on the activation of T cell responses against DTH response. Online supplemental material is available at http://www.jem.org/cgi/content/full/jem.20090397/DC1.

We thank Dr. Q. Ao and Dr. C. Ke for reviewing histology data, Dr. Y. Tong for assisting in tissue sample collection, and Professor J.Y. Niederkorn and Dr. Z. Feng for inspiration and discussion.

This work was supported by the National Science Foundation of China (grants 30770914 and 30901587) and the "973" Program (grant 2009CB521800).

The authors have no conflicting financial interests.

Submitted: 19 February 2009
Accepted: 25 January 2010

REFERENCES

Bai, X., M. Huang, J. Wu, X. Huang, L. Yan, Y. Lu, S. Wang, G. Xu, J. Zhou, and D. Ma. 2008. Development and characterization of a novel method to analyze global gene expression profiles in endothelial cells derived from primary tissues. *Am. J. Hematol.* 83:26–33. doi:10.1002/ajh.20953

Bruns, I., F. Fox, P. Reinecke, G. Kobbe, R. Kronenwett, G. Jung, and R. Haas. 2005. Complete remission in a patient with relapsed angioimmunoblastic T-cell lymphoma following treatment with bevacizumab. *Leukemia.* 19:1993–1995. doi:10.1038/sj.leu.2403936

Choi, J., D.R. Enis, K.P. Koh, S.L. Shiao, and J.S. Pober. 2004. T lymphocyte-endothelial cell interactions. *Annu. Rev. Immunol.* 22: 683–709. doi:10.1146/annurev.immunol.22.012703.104639

Cooke, B.M., S. Usami, I. Perry, and G.B. Nash. 1993. A simplified method for culture of endothelial cells and analysis of adhesion of blood cells under conditions of flow. *Microvasc. Res.* 45:33–45. doi:10.1006/mvre.1993.1004

Coupel, S., F. Leboeuf, G. Boulday, J.P. Soulillou, and B. Charreau. 2004. RhoA activation mediates phosphatidylinositol 3-kinase-dependent proliferation of human vascular endothelial cells: an alloimmune mechanism of chronic allograft nephropathy. *J. Am. Soc. Nephrol.* 15:2429–2439. doi:10.1097/01.ASN.0000138237.42675.45

Coventry, B.J., and J. Morton. 2003. CD1a-positive infiltrating-dendritic cell density and 5-year survival from human breast cancer. *Br. J. Cancer.* 89:533–538. doi:10.1038/sj.bjc.6601114

Danese, S., E. Dejana, and C. Fiocchi. 2007. Immune regulation by microvascular endothelial cells: directing innate and adaptive immunity, coagulation, and inflammation. *J. Immunol.* 178:6017–6022.

Fidler, I.J., and L.M. Ellis. 2004. Neoplastic angiogenesis–not all blood vessels are created equal. *N. Engl. J. Med.* 351:215–216. doi:10.1056/NEJMp048080

Gao, Q., X. Huang, D. Tang, Y. Cao, G. Chen, Y. Lu, L. Zhuang, S. Wang, G. Xu, J. Zhou, and D. Ma. 2006. Influence of chk1 and plk1 silencing on radiation- or cisplatin-induced cytotoxicity in human malignant cells. *Apoptosis.* 11:1789–1800. doi:10.1007/s10495-006-9421-4

Gao, D., D.J. Nolan, A.S. Mellick, K. Bambino, K. McDonnell, and V. Mittal. 2008. Endothelial progenitor cells control the angiogenic switch in mouse lung metastasis. *Science.* 319:195–198. doi:10.1126/science.1150224

Geng, H., G.M. Zhang, D. Li, H. Zhang, Y. Yuan, H.G. Zhu, H. Xiao, L.F. Han, and Z.H. Feng. 2006. Soluble form of T cell Ig mucin 3 is an inhibitory molecule in T cell-mediated immune response. *J. Immunol.* 176:1411–1420.

Göthert, J.R., S.E. Gustin, J.A. van Eekelen, U. Schmidt, M.A. Hall, S.M. Jane, A.R. Green, B. Göttgens, D.J. Izon, and C.G. Begley. 2004. Genetically tagging endothelial cells in vivo: bone marrow-derived cells do not contribute to tumor endothelium. *Blood.* 104:1769–1777. doi:10.1182/blood-2003-11-3952

Gunsilius, E., H.C. Duba, A.L. Petzer, C.M. Kähler, K. Grünewald, G. Stockhammer, C. Gabl, S. Dirnhofer, J. Clausen, and G. Gastl. 2000. Evidence from a leukaemia model for maintenance of vascular endothelium by bone-marrow-derived endothelial cells. *Lancet.* 355:1688–1691. doi:10.1016/S0140-6736(00)02241-8

Karnoub, A.E., A.B. Dash, A.P. Vo, A. Sullivan, M.W. Brooks, G.W. Bell, A.L. Richardson, K. Polyak, R. Tubo, and R.A. Weinberg. 2007. Mesenchymal stem cells within tumour stroma promote breast cancer metastasis. *Nature.* 449:557–563. doi:10.1038/nature06188

Kim, R., M. Emi, K. Tanabe, and K. Arihiro. 2006. Tumor-driven evolution of immunosuppressive networks during malignant progression. *Cancer Res.* 66:5527–5536. doi:10.1158/0008-5472.CAN-05-4128

Koster, A., and J.M. Raemaekers. 2005. Angiogenesis in malignant lymphoma. *Curr. Opin. Oncol.* 17:611–616. doi:10.1097/01.cco.0000181404.83084.b5

Kuchroo, V.K., D.T. Umetsu, R.H. DeKruyff, and G.J. Freeman. 2003. The TIM gene family: emerging roles in immunity and disease. *Nat. Rev. Immunol.* 3:454–462. doi:10.1038/nri1111

Lenz, G., G. Wright, S.S. Dave, W. Xiao, J. Powell, H. Zhao, W. Xu, B. Tan, N. Goldschmidt, J. Iqbal, et al. 2008. Stromal gene signatures in large-B-cell lymphomas. *N. Engl. J. Med.* 359:2313–2323.

Maloney, D.G. 2005. Immunotherapy for non-Hodgkin's lymphoma: monoclonal antibodies and vaccines. *J. Clin. Oncol.* 23:6421–6428. doi:10.1200/JCO.2005.06.004

Neri, D., and R. Bicknell. 2005. Tumour vascular targeting. *Nat. Rev. Cancer.* 5:436–446. doi:10.1038/nrc1627

Nobumoto, A., K. Nagahara, S. Oomizu, S. Katoh, N. Nishi, K. Takeshita, T. Niki, A. Tominaga, A. Yamauchi, and M. Hirashima. 2008. Galectin-9 suppresses tumor metastasis by blocking adhesion to endothelium and extracellular matrices. *Glycobiology.* 18:735–744. doi:10.1093/glycob/cwn062

Padua, R.A., J. Larghero, M. Robin, C. le Pogam, M.H. Schlageter, S. Muszlak, J. Fric, R. West, P. Rousselot, T.H. Phan, et al. 2003. PML-RARA-targeted DNA vaccine induces protective immunity in a mouse model of leukemia. *Nat. Med.* 9:1413–1417. doi:10.1038/nm949

Pezzolo, A., F. Parodi, M.V. Corrias, R. Cinti, C. Gambini, and V. Pistoia. 2007. Tumor origin of endothelial cells in human neuroblastoma. *J. Clin. Oncol.* 25:376–383. doi:10.1200/JCO.2006.09.0696

Rice, J., T. Elliott, S. Buchan, and F.K. Stevenson. 2001. DNA fusion vaccine designed to induce cytotoxic T cell responses against defined peptide motifs: implications for cancer vaccines. *J. Immunol.* 167:1558–1565.

Rigolin, G.M., C. Fraulini, M. Ciccone, E. Mauro, A.M. Bugli, C. De Angeli, M. Negrini, A. Cuneo, and G. Castoldi. 2006. Neoplastic

circulating endothelial cells in multiple myeloma with 13q14 deletion. *Blood*. 107:2531–2535. doi:10.1182/blood-2005-04-1768

Sabatos, C.A., S. Chakravarti, E. Cha, A. Schubart, A. Sánchez-Fueyo, X.X. Zheng, A.J. Coyle, T.B. Strom, G.J. Freeman, and V.K. Kuchroo. 2003. Interaction of Tim-3 and Tim-3 ligand regulates T helper type 1 responses and induction of peripheral tolerance. *Nat. Immunol.* 4:1102–1110. doi:10.1038/ni988

Sánchez-Fueyo, A., J. Tian, D. Picarella, C. Domenig, X.X. Zheng, C.A. Sabatos, N. Manlongat, O. Bender, T. Kamradt, V.K. Kuchroo, et al. 2003. Tim-3 inhibits T helper type 1-mediated auto- and alloimmune responses and promotes immunological tolerance. *Nat. Immunol.* 4:1093–1101. doi:10.1038/ni987

Shih, S.C., and K.P. Claffey. 1999. Regulation of human vascular endothelial growth factor mRNA stability in hypoxia by heterogeneous nuclear ribonucleoprotein L. *J. Biol. Chem.* 274:1359–1365. doi:10.1074/jbc.274.3.1359

Song, D., S. Sakamoto, and T. Taniguchi. 2002. Inhibition of poly(ADP-ribose) polymerase activity by Bcl-2 in association with the ribosomal protein S3a. *Biochemistry*. 41:929–934. doi:10.1021/bi015669c

Steeg, P.S., and D. Theodorescu. 2008. Metastasis: a therapeutic target for cancer. *Nat. Clin. Pract. Oncol.* 5:206–219. doi:10.1038/ncponc1066

Streubel, B., A. Chott, D. Huber, M. Exner, U. Jäger, O. Wagner, and I. Schwarzinger. 2004. Lymphoma-specific genetic aberrations in microvascular endothelial cells in B-cell lymphomas. *N. Engl. J. Med.* 351:250–259. doi:10.1056/NEJMoa033153

Sun, Y., M. Song, E. Jäger, C. Schwer, S. Stevanovic, S. Flindt, J. Karbach, X.D. Nguyen, D. Schadendorf, and K. Cichutek. 2008. Human CD4+ T lymphocytes recognize a vascular endothelial growth factor receptor-2-derived epitope in association with HLA-DR. *Clin. Cancer Res.* 14:4306–4315. doi:10.1158/1078-0432.CCR-07-4849

Tiemessen, M.M., A.L. Jagger, H.G. Evans, M.J. van Herwijnen, S. John, and L.S. Taams. 2007. CD4+CD25+Foxp3+ regulatory T cells induce alternative activation of human monocytes/macrophages. *Proc. Natl. Acad. Sci. USA*. 104:19446–19451. doi:10.1073/pnas.0706832104

van Dongen, J.J., A.W. Langerak, M. Brüggemann, P.A. Evans, M. Hummel, F.L. Lavender, E. Delabesse, F. Davi, E. Schuuring, R. García-Sanz, et al. 2003. Design and standardization of PCR primers and protocols for detection of clonal immunoglobulin and T-cell receptor gene recombinations in suspect lymphoproliferations: report of the BIOMED-2 Concerted Action BMH4-CT98-3936. *Leukemia*. 17:2257–2317. doi:10.1038/sj.leu.2403202

van Krieken, J.H., A.W. Langerak, E.A. Macintyre, M. Kneba, E. Hodges, R.G. Sanz, G.J. Morgan, A. Parreira, T.J. Molina, J. Cabeçadas, et al. 2007. Improved reliability of lymphoma diagnostics via PCR-based clonality testing: report of the BIOMED-2 Concerted Action BHM4-CT98-3936. *Leukemia*. 21:201–206. doi:10.1038/sj.leu.2404467

Weidner, N. 1995. Intratumor microvessel density as a prognostic factor in cancer. *Am. J. Pathol.* 147:9–19.

Wong, O.H., F.P. Huang, and A.K. Chiang. 2005. Differential responses of cord and adult blood-derived dendritic cells to dying cells. *Immunology*. 116:13–20. doi:10.1111/j.1365-2567.2005.02191.x

Wu, J., L. Huang, M. Huang, W. Liu, M. Zheng, Y. Cao, Y. Liu, Y. Zhang, Y. Lu, G. Xu, et al. 2009. Dominant contribution of malignant endothelial cells to endotheliopoiesis in chronic myeloid leukemia. *Exp. Hematol.* 37:87–91. doi:10.1016/j.exphem.2008.08.009

Zhou, J., Q. Gao, G. Chen, X. Huang, Y. Lu, K. Li, D. Xie, L. Zhuang, J. Deng, and D. Ma. 2005. Novel oncolytic adenovirus selectively targets tumor-associated polo-like kinase 1 and tumor cell viability. *Clin. Cancer Res.* 11:8431–8440. doi:10.1158/1078-0432.CCR-05-1085

Zhu, C., A.C. Anderson, A. Schubart, H. Xiong, J. Imitola, S.J. Khoury, X.X. Zheng, T.B. Strom, and V.K. Kuchroo. 2005. The Tim-3 ligand galectin-9 negatively regulates T helper type 1 immunity. *Nat. Immunol.* 6:1245–1252. doi:10.1038/ni1271